Decay of an ion temperature discontinuity in a collisionless plasma

Article *in* Plasma Physics and Controlled Fusion · January 1999

DOI: 10.1088/0741-3335/35/9/003

1 author:

Yury Vasilevich Medvedev
Joint Institute for High Temperatures
37 PUBLICATIONS **437** CITATIONS

Plasma Phys. Control. Fusion 35 (1993) 1103–1118. Printed in the UK

Decay of an ion temperature discontinuity in a collisionless plasma

Yu V Medvedev
Institute for High Temperatures of Russian Academy of Sciences, Moscow, 127412, Russia

Received 31 March 1992, in final form 19 March 1993

Abstract. The decay of an ion temperature discontinuity in a collisionless plasma is considered. Theoretical analysis and simulation are used. It is shown that a shock is formed in the cold plasma region and a rarefraction wave is formed in the hot plasma region. Profiles of density and potential are presented. A comparison of the theoretical dependence on the initial hot ion temperature of the hot ion density, temperature, velocity, current and energy flux at the plateau region and the shock speed with the simulation data shows good agreement.

1. Introduction

The decay of an arbitrary initial discontinuity of some parameters is an important problem in hydrodynamics (Landau and Lifshits 1986). The same problem arises in kinetics. The first investigation of discontinuity decay in plasma kinetics was carried out by Gurevich *et al* (1966), and a self-similar solution of the collisionless kinetic equation has been described for the case of plasma expansion into a vacuum. This process, and the more general problem on the evolution of an arbitrary discontinuity of plasma density, were both later studied in further detail (Allen and Andrews 1970, Mason 1970, 1971, Gurevich and Pitaevskii 1975, Anisimov and Medvedev 1979, Denavit 1979, 1981, Gurevich and Meschcrkin 1984, Sack and Schamel 1987, Gurevich *et al* 1989).

The evolution of a flow velocity discontinuity has also been considered, both in the hydrodynamic approximation (Gurevich and Meshcherkin 1984) and in the frame of collisionless plasma kinetics (Gurevich and Medvedev 1989, 1990, 1992).

Contrary to the decay of a density discontinuity, the decay of an initial discontinuity of ion or electron temperature is less well studied, although there are situations in which two plasmas with different temperatures are in contact with each other. For instance, in a tandem mirror machine the cool central-cell plasma contacts with the hot plug-cell plasma, and some problems arise such as thermal insulation, formation of a thermal barrier, control of particle and energy fluxes and so on (Dimov *et al* 1976, Baldwin and Logan 1979, Ohkawa *et al* 1983).

Another example is the interaction of the hot magnetosphere plasma and the cold ionosphere plasma that produces a magnetic-field-aligned electric field (Hultqvist 1971). Such fields have been observed (Temerin *et al* 1982); they can be responsible for the acceleration of auroral particles. In connection with these

0741-3335/93/091103+16 $07.50

investigations the formation of an electrostatic potential barrier between two plasmas with different electron temperatures and ion species has been studied in a Q-machine experiment (Hatakeyama *et al*, 1983).

Large gradients of electron temperature can be developed in a laser plasma. In recent years the problem of energy transport in such a plasma has attracted considerable interest (Malone *et al* 1975, Gitomer and Henderson 1979, Braithwaite *et al* 1981).

For the purpose of calculating the upper limit of energy flux in a collisionless plasma the decay of an electron temperature discontinuity has been studied (Medvedev 1979a,b).

The simultaneous decays of the ion and electron temperature discontinuities have been considered, provided that the initial pressure of each plasma component is continuous (Ishiguro *et al* 1985, Ishiguro 1987). The structure of the potential profiles and the energy flux have been examined. It is noteworthy that the value of the electron energy flux obtained (Ishiguro 1987) coincides with the upper limit of the energy flux found earlier (Medvedev 1979b).

In the present paper the decay of an initial ion temperature discontinuity is considered. The electron temperature is assumed to be continuous. In section 2 the formulation of the problem and a theoretical analysis are given. Numerical simulation results are presented in section 3. In section 4 there is a discussion, and, finally, a summary is given in section 5.

2. Theoretical analysis

2.1. Basic equations

Let us consider a collisionless plasma that consists of two species of ions, cold and hot. Ions of both species are identical in charge and mass. The difference between two species of ions is in their initial states. At time $t=0$ the cold ions have a Maxwellian velocity distribution with temperature T_{c0} and occupy the half-space $-\infty<x<0$. The hot ions have the same distribution except that temperature is equal to T_{h0}. They occupy the half-space $0<x<\infty$. The initial number density of ions of both species is n_{i0} and the initial electron number density is n_{e0}; n_{i0} and n_{e0} are constant for $-\infty<x<\infty$. The quasineutrality condition implies that $n_{e0}=Zn_{i0}$, where Ze is the ion charge and $-e$ is the electron charge. The electron temperature T_e remains constant during the process. In other words, at $t=0$ an initial discontinuity of ion temperature is given at a point $x=0$.

It is apparent that the characteristic velocity scale of the process is determined by ions. In such a case a one-dimensional plasma motion is described (Lifshits and Pitaevskii 1979) by the kinetic equation for the ion distribution function $f_i(x,v,t)$:

$$\frac{\partial f_i}{\partial t}+v\frac{\partial f_i}{\partial x}-\frac{Ze}{m_i}\frac{\partial \phi}{\partial x}\frac{\partial f_i}{\partial v}=0 \tag{1}$$

and Poisson's equation for the electrostatic potential $\phi(x,t)$:

$$\frac{\partial^2\phi}{\partial x^2}=-4\pi e(Zn_i-n_e), \tag{2}$$

where

$$n_i = \int_{-\infty}^{\infty} f_i(x, v, t)\, dv \tag{3}$$

and

$$n_e = n_{e0} \exp(e\phi / T_e) \tag{4}$$

are the ion and electron number densities, respectively, m_i is an ion mass, v is velocity and T_e is given in energy units. The electrons are assumed to obey Boltzmann's law.

The set of equations (1)–(4) with appropriate initial and boundary conditions can be solved by a numerical simulation. However, it is useful to consider some approximations. In particular, the closed set of equations for the first three moments of the distribution function can be obtained on the assumption that thermal flux is equal to zero (Gurevich and Pitaevskii 1975, Gurevich *et al* 1989):

$$\frac{\partial n_i}{\partial t} + V_i \frac{\partial n_i}{\partial x} + n_i \frac{\partial V_i}{\partial x} = 0 \tag{5}$$

$$\frac{\partial V_i}{\partial t} + V_i \frac{\partial V_i}{\partial x} + \frac{1}{n_i m_i} \frac{\partial}{\partial x}(n_i T_i) + \frac{Ze}{m_i} \frac{\partial \phi}{\partial x} = 0 \tag{6}$$

$$\frac{\partial T_i}{\partial t} + V_i \frac{\partial T_i}{\partial x} + 2T_i \frac{\partial V_i}{\partial x} = 0 \tag{7}$$

where

$$V_i = \frac{1}{n_i} \int_{-\infty}^{\infty} v f_i(x, v, t)\, dv \qquad T_i = \frac{m_i}{n_i} \int_{-\infty}^{\infty} (v - V_i)^2 f_i(x, v, t)\, dv.$$

These equations must be supplemented by equations (2) and (4).

It is easy to verify that equations (5) and (7) have the integral (Gurevich and Pitaevskii 1975)

$$T_i / n_i^2 = T_{i0} / n_{i0}^2 = \text{const.} \tag{8}$$

Clearly, equation (7) can be replaced by equation (8).

2.2. *Neutral approximation*

Due to the lack of literature on the problem under investigation the simplest case will be our initial concern. For a qualitative analysis we use the assumption of full neutrality $n_e \equiv Zn_i$. In such a case equations (2) and (4) can be dropped and the last term in equation (6) can be neglected. In this approximation electric forces are absent and ions are identical to neutral particles. Because of this let us denote

$$P = n_i T_i \qquad \rho = m_i n_i$$

and omit the subscript i in equations (5), (6) and (8) for this subsection. We have

$$\frac{\partial \rho}{\partial t} + V \frac{\partial \rho}{\partial x} + \rho \frac{\partial V}{\partial x} = 0 \tag{9}$$

$$\frac{\partial V}{\partial t} + V \frac{\partial V}{\partial x} + \frac{1}{\rho} \frac{\partial P}{\partial x} = 0 \tag{10}$$

$$T = T_0 \rho^2 / \rho_0^2. \tag{11}$$

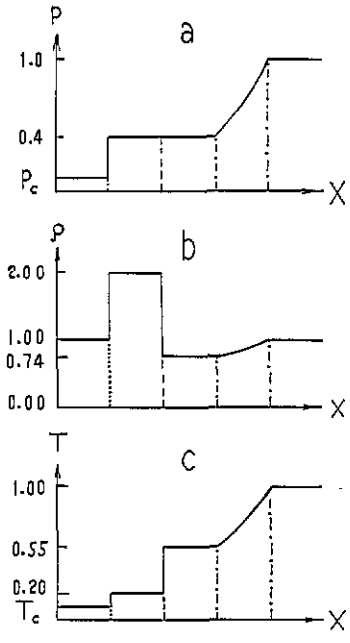

Figure 1. Schematic views of profiles of pressure P, density ρ and temperature T. P, ρ and T are normalized to P_{h0}, ρ_{h0} and T_{h0}, respectively. The dotted, dashed and chain lines represent the shock, the contact surface and the weak discontinuities, respectively.

These equations coincide with the hydrodynamic ones for a one-dimensional motion of an ideal gas with the adiabatic exponent $\gamma = 3$.

Thermal expansion of a contact surface between two species of particles cannot be studied in the frame of hydrodynamic equations (9)–(11). The contact surface does not disappear and two gases do not mix together during the process. But a temperature discontinuity gives a pressure discontinuity since the density is continuous in our case. Pressure discontinuity is already a subject of investigation in hydrodynamics.

It is well known (Landau and Lifshits 1986) that the decay of an initial pressure discontinuity occurs in such a way that a shock moves into the low-pressure gas and a rarefaction wave moves into the high-pressure gas. A plateau region with constant pressure is set up between the shock and the rarefaction wave. There is a tangential discontinuity between two gases at this region. In our case the tangential discontinuity degenerates into a contact discontinuity. The rarefaction wave is bounded by two weak discontinuities. The first weak discontinuity is at the point of contact of the plateau region and the rarefaction wave, and the second weak discontinuity joins the rarefaction wave to the hot undisturbed gas (Figure 1(*a*)).

We denote quantities of the cold and hot undisturbed gases by the subscripts c0 and h0, respectively. Quantities are specified by two subscripts c and p at the region between the shock and the contact discontinuity, and two subscripts h and p are used in the remainder of the plateau region.

To find the profiles of hydrodynamic variables we use relations between the variables at the shock, at the contact discontinuity and at the weak discontinuities (Landau and Lifshits 1986).

At the shock the Hugoniot adiabat can be written as

$$\frac{\rho_{c0}}{\rho_{cp}} = \frac{(\gamma+1)P_{c0} + (\gamma-1)P_{cp}}{(\gamma-1)P_{c0} + (\gamma+1)P_{cp}}. \tag{12}$$

The velocity behind the shock with reference to the cold gas is given by

$$V_{cp} = -[(P_{cp} - P_{c0})(\rho_{c0}^{-1} - \rho_{cp}^{-1})]^{1/2}. \tag{13}$$

The pressure and velocity must be continuous at the contact discontinuity and we have

$$P_{cp} = P_{hp} \qquad V_{cp} = V_{hp}. \tag{14}$$

The velocity is continuous at the first weak discontinuity. This condition can be written as

$$V_{hp} = \frac{2}{\gamma - 1} c_{h0}\left[\left(\frac{P_{hp}}{P_{h0}}\right)^{(\gamma-1)/2\gamma} - 1\right] \tag{15}$$

where

$$c_{h0} = (\gamma P_{h0}/\rho_{h0})^{1/2}$$

is the acoustic speed of the undisturbed hot gas.

Using equations (12) and (13) we can obtain, after some algebra,

$$\frac{P_{cp}}{P_{h0}} = \frac{P_{c0}}{P_{h0}} + \frac{\gamma(\gamma+1)}{4}\frac{\rho_{c0}}{\rho_{h0}}u^2 + \gamma u\left[\frac{\rho_{c0}}{\rho_{h0}}\left(\frac{P_{c0}}{P_{h0}} + \frac{(\gamma+1)^2}{16}\frac{\rho_{c0}}{\rho_{h0}}u^2\right)\right]^{1/2} \tag{16}$$

where we denote

$$u = V_{cp}/c_{h0}.$$

On the other hand, the same quantity can be found from equations (14) and (15) as

$$\frac{P_{cp}}{P_{h0}} = \left(1 + \frac{\gamma - 1}{2}u\right)^{2\gamma/(\gamma-1)}. \tag{17}$$

Equating the right-hand sides of equations (16) and (17) we can obtain an equation with one unknown u. When a solution to this equation is found we can evaluate all quantities and construct profiles.

In our case $\rho_{c0} = \rho_{h0}$ and $\gamma = 3$ we have

$$\frac{P_{c0}}{P_{h0}} + 3u^2 + 3u(u^2 + P_{c0}/P_{h0})^{1/2} = (1+u)^3. \tag{18}$$

For the purposes of illustration we consider a case of strong shock $P_{h0} \gg P_{c0}$. Then equation (18) can be rewritten as

$$6u^2 = (1+u)^3. \tag{19}$$

The root of equation (19) is

$$u \simeq -0.26. \tag{20}$$

Next, using equations (17), (14), (11) and known relations for a strong shock in an ideal gas (Landau and Lifshits 1986):

$$\frac{\rho_{c0}}{\rho_{cp}} = \frac{\gamma - 1}{\gamma + 1} \qquad \frac{T_{cp}}{T_{c0}} = \frac{\gamma - 1}{\gamma + 1}\frac{P_{cp}}{P_{c0}} \qquad \frac{w^2}{c_{c0}^2} = \frac{\gamma + 1}{2\gamma}\frac{P_{cp}}{P_{c0}}$$

where

$$c_{c0} = (\gamma P_{c0}/\rho_{c0})^{1/2}$$

is the acoustic speed of the undisturbed cold gas and w is the shock speed relative to the cold gas, we obtain, after some calculations,

$$V_{cp} = V_{hp} \simeq -0.26c_{h0} \qquad P_{cp} = P_{hp} \simeq 0.4P_{h0}$$
$$\rho_{cp} = 2\rho_{h0} \qquad \rho_{hp} \simeq 0.74\rho_{h0} \qquad T_{cp} \simeq 0.2T_{h0} \tag{21}$$
$$T_{hp} \simeq 0.55T_{h0} \qquad w \simeq -0.516(P_{h0}/P_{c0})^{1/2}c_{c0}.$$

Hence we have a solution at the plateau region.

Let us designate quantities at the rarefaction wave region by subscript h and write the known relations (Landau and Lifshits 1986):

$$|V_h| = \frac{2}{\gamma+1}\left(c_{h0} - \frac{x}{t}\right) \qquad \rho_h = \rho_{h0}\eta^{2/(\gamma-1)}$$
$$P_h = P_{h0}\eta^{2\gamma/(\gamma-1)} \qquad T_h = T_{h0}\eta^2$$

where

$$\eta = 1 - \frac{\gamma-1}{2}\frac{|V_h|}{c_{h0}}.$$

For our case the solution at the rarefraction wave region can be written as

$$|V_h| = 0.5(c_{h0} - x/t) \qquad \eta = 1 - |V_h|/c_{h0} \tag{22}$$
$$\rho_h = \rho_{h0}\eta \qquad P_h = P_{h0}\eta^3 \qquad T_h = T_{h0}\eta^2.$$

The profiles of density and temperature are illustrated schematically in figures 1(b) and 1(c). The formation of a density hump and a following dip in density is an essential element of the process.

It is interesting to note that a similar density profile structure can be observed in the opposite case, namely, in a system of free particles. The decay of the temperature discontinuity in that system takes place due to the relative permeation of particles. The hot particles move more quickly than the cold ones and form an excess of particles at the region initially occupied by the cold particles. The cold particles do not compensate for a lack of particles in the region initially occupied by the hot particles. As a result the density profile has a hump and a following dip near the initial position of the discontinuity (Medvedev 1979a).

The main difference between two cases is in the means of formation of the density hump.

2.3. *Quasineutral approximation*

When characteristic lengths of motion are much more than the Debye length the quasineutral approximation can be used (Gurevich *et al* 1966, Gurevich and Pitaevskii 1975). In this case the motion turns out to be self-similar; the left side of equation (2) can be neglected and from equations (2) and (4) we have

$$\phi = \frac{T_e}{e}\ln\frac{n_i}{n_{i0}}. \tag{23}$$

Defining the self-similar variable $\tau = x/t$ we can write equations (5), (6), (8) and (23) as

$$(V_i - \tau)\frac{dn_i}{d\tau} + n_i\frac{dV_i}{d\tau} = 0 \tag{24}$$

$$(V_i - \tau)\frac{dV_i}{d\tau} + \frac{1}{m_i n_i}\frac{dP}{d\tau} = 0 \tag{25}$$

$$P = ZT_e n_i + \frac{T_{i0}}{n_{i0}^2} n_i^3. \tag{26}$$

The distinctive property of the set of equations (24)–(26) is that they take into consideration the ion pressure in the equation of state (26).

Using standard practice (Landau and Lifshits 1986) we eliminate derivatives from equations (24) and (25) and obtain

$$V_i - \tau = \pm c_i(n_i) \tag{27}$$

where

$$c_i(n_i) = \left(\frac{ZT_e}{m_i} + \frac{3T_{i0}}{m_i}\frac{n_i^2}{n_{i0}^2}\right)^{1/2}. \tag{28}$$

Substituting equation (27) in equation (24) we have

$$dV_i = \pm\frac{c_i(n_i)}{n_i} dn_i$$

which on integration gives

$$V_i - V_{i0} = \pm\left[c_i - c_{i0} + \tfrac{1}{2}c_e\left(\ln\frac{c_i - c_e}{c_i + c_e} - \ln\frac{c_{i0} - c_e}{c_{i0} + c_e}\right)\right] \tag{29}$$

where

$$c_e = (ZT_e/m_i)^{1/2} \qquad c_{i0} = c_e(1 + 3T_{i0}/ZT_e)^{1/2}. \tag{30}$$

An implicit relation between n_i and τ can be found from equations (27)–(29) and we can obtain $n_i(\tau)$ and subsequently $V_i(\tau)$ and $P(\tau)$. It is self-evident that equations (24)–(26) also have simple solutions in a plateau form

$$n_i = \text{const}_1 \qquad V_i = \text{const}_2 \qquad P = \text{const}_3. \tag{31}$$

However, a full solution of the problem cannot be constructed with only equations (27)–(31). To remedy this, another type of solution must be allowed. A shock is used in a similar case in hydrodynamics. In the case of collisionless plasma a quasistationary wave fulfils the role of a shock. The quasistationary wave is a discontinuity of a special kind. Its structure is determined by dispersion. The wave expands linearly with time and hence is called the self-similar discontinuity (Gurevich and Meshcherkin 1984).

The introduction of the concept of such a discontinuity makes it possible to construct a full solution everywhere over the region except the discontinuity. For this purpose we must set a relation between the variables on both sides of the discontinuity similar to the Hugoniot adiabat in hydrodynamics. In the case of cold ions $T_{i0} = 0$ this relation for the discontinuity moving in the direction of negative x takes the form (Gurevich and Meshcherkin 1984):

$$V_i - V_{i0} = -c_e \ln(n_i/n_{i0}) \tag{32}$$

where V_{i0} and n_{i0} fall in the region ahead of the wave and V_i and n_i do in the region behind the wave. An important point is that the relation (32) is true only for a dissipationless case and the quasistationary wave can be called the dissipationless shock. It is because of the lack of dissipation that equation (32) can be derived from the continuous solution.

It is easily shown that equation (29) rearranges to equation (32) in the case $T_{i0} = 0$. In other words, equation (29) is a generalization of the relation (32) to the case $T_{i0} \neq 0$.

Thereafter it becomes evident that taking two species of ions do not mix together in the course of decay, we can find a solution at the plateau region and at the rarefaction wave in much the same way as the consideration in the earlier subsection.

Before we proceed further, let us normalize all variables and by this means simplify the consideration. We take the Debye length D, c_e, the values of D/c_e, ZT_e, $ZT_e n_{e0}$ and n_{e0} as the scales of length, velocity, time, temperature, pressure and density, respectively. Henceforth all quantities are given in normalized form. Notation remains as before. Moreover we use the subscript notation of the previous subsection. We assume for simplicity $n_{c0} = n_{h0} = n_{e0}$.

Next, expressing equations (28)–(30) in terms of the above normalized variables, we obtain a relation for the variables on both sides of the dissipationless shock as

$$V_{cp} = -c_{cp} + c_{c0} - \frac{1}{2}\left(\ln\frac{c_{cp}-1}{c_{cp}+1} - \ln\frac{c_{c0}-1}{c_{c0}+1}\right) \qquad (33)$$
$$c_{cp} = (1 + 3T_{c0}n_{cp}^2)^{1/2} \qquad c_{c0} = (1 + 3T_{c0})^{1/2}.$$

Equations (14) are fulfilled at the contact discontinuity. Using equations (28)–(30) at the first weak discontinuity we have

$$V_{hp} = c_{hp} - c_{h0} + \frac{1}{2}\left(\ln\frac{c_{hp}-1}{c_{hp}+1} - \ln\frac{c_{h0}-1}{c_{h0}+1}\right) \qquad (34)$$
$$c_{hp} = (1 + 3T_{h0}n_{hp}^2)^{1/2} \qquad c_{h0} = (1 + 3T_{h0})^{1/2}.$$

From equation (14) for pressure and equation (26) we have

$$n_{cp} + T_{c0}n_{cp}^3 = n_{hp} + T_{h0}n_{hp}^3. \qquad (35)$$

As can be seen from equations (33) and (34) we can treat the quantities V_{cp} and V_{hp} as functions of density and temperature and write equation (14) for velocity symbolically

$$V_{cp}(T_{c0}, n_{cp}) = V_{hp}(T_{h0}, n_{hp}). \qquad (36)$$

As a result we have a set of two equations (35) and (36) in two variables n_{cp} and n_{hp}. Two parameters T_{c0} and T_{h0} are involved in the equations.

Let us restrict our consideration to a single but important case $T_{c0} \to 0$. Under this assumption a single parameter T_{h0} is in the equations. In the cold plasma only the pressure of electrons is taken into account. We have from equations (33)

$$V_{cp} = -\ln n_{cp} \qquad (37)$$

that is equation (32) in normalized form. Equations (34)–(37) may be rearranged to

give

$$(1+3T_{h0}n_{hp}^2)^{1/2}+\frac{1}{2}\ln\frac{(1+3T_{h0}n_{hp}^2)^{1/2}-1}{(1+3T_{h0}n_{hp}^2)^{1/2}+1}+\ln(n_{hp}+T_{h0}n_{hp}^3)$$
$$=(1+3T_{h0})^{1/2}+\frac{1}{2}\ln\frac{(1+3T_{h0})^{1/2}-1}{(1+3T_{h0})^{1/2}+1}. \tag{38}$$

At given T_{h0} equation (38) can be solved for the unknown density n_{hp}. Thereafter we can evaluate all quantities at the plateau region.

As noted above, the dependence of all quantities on τ at the rarefaction wave region can be obtained from equations (27)–(29). The position of the first weak discontinuity is determined by joining solutions at the rarefaction wave region and at the plateau one. The second weak discontinuity position is at

$$x_2=t(1+3T_{h0})^{1/2}.$$

Results of numerical solutions of equations (38) and (27)–(29) will be considered in combination with simulation data.

2.4. Shock speed

The quasineutral approximation is broken down at the dissipationless shock. The detailed structure of a shock has been considered (Gurevich and Meshcherkin 1984, Gurevich *et al* 1989) and we restrict ourselves to the determination of shock speed, the final parameter required for a construction of profiles.

The shock speed is in fact the speed of the leading soliton of the shock which depends on the soliton potential amplitude. In the case of cold ions this dependence has been obtained (Sagdeev 1966). But we cannot use it because the soliton amplitude is unknown in our approximation.

Instead, an alternative method is feasible. There is a one-to-one correspondence between the shock speed and ratio of the densities at the plateau region and at the region ahead of the shock:

$$w=w(n_{cp}/n_{c0}).$$

This dependence has been established in the frame of the hydrodynamic approach (Gurevich and Meshcherkin 1984) and has then been examined by means of the kinetic numerical simulation (Gurevich *et al* 1989). It has been presented in the form of a curve.

We derive the shock speed from this curve using the value of n_{cp}/n_{c0} obtained in the previous subsection. Results of calculations are shown in figure 7.

3. Simulation

A particle-in-cell computer simulation (Hockney and Eastwood 1981) is used to study the decay of an ion temperature discontinuity. The ions are simulated by particles, which move in the electric field in accordance with equations of motion that are identical with equations of the characteristics of the kinetic equation (1). The electric field is found at each point in time by solving Poisson's equation (2)–(4). The values of electric field at the boundaries of the simulation region are assumed to be equal to zero. Reflection conditions are set for the particles at the

boundaries. Under these conditions, the plasma state can be kept homogeneous close to the boundaries, as long as no disturbance reaches them. Such is indeed the case since systems studied are from 600 to 1200 Debye lengths long and the upper time limit considered is $350(D/c_e)$.

In addition to the scales of quantities introduced in the previous section, we use the values of T_e/e, $Zen_{e0}(T_e/m_i)^{1/2}$ and $(1/2)n_{e0}T_e(T_e/m_i)^{1/2}$ as the scales of potential, ion current and energy flux, respectively.

We have performed a series of the simulation runs for different initial temperatures of the hot and cold ions. Taking into account the results of theoretical analysis the runs can be classified according to T_{h0}. We have used the following values of T_{h0}: 0.05, 0.1, 0.25, 0.5 and 1. At each given T_{h0} two cases have been considered: $T_{c0} = 0.001$ and $T_{c0} = 0.01$. In addition, we have used $T_{c0} = 0.1$ for the cases $T_{h0} = 0.5$ and $T_{h0} = 1$.

Some results of simulation are plotted as functions of T_{h0}. In such cases data are averaged over the runs with the same T_{h0}.

3.1. Structure of flow

The decay of an ion temperature discontinuity occurs in such a way that a density hump is formed in the cold ion region $x < 0$ and a dip in density is formed in the hot ion region $x > 0$. The compression wave moves as a shock into the cold ion region and the rarefaction wave does so into the hot ion region. The rarefaction wave is followed by the short plateau range (figure 2). This is true for any relation between T_{c0} and T_{h0}.

No density discontinuity forms between two species of ions. Either of the two ion species penetrates into the region occupied by another species. The initial contact discontinuity turns out to be expanded. Nevertheless, the approximate analysis of the previous section provides a rather correct description of the shock front and the plateau and rarefaction wave regions. The weak discontinuities which bound the rarefaction wave appear to be somewhat expanded by thermal motion. There is a small-amplitude compression wave ahead of the shock front. This wave is made up

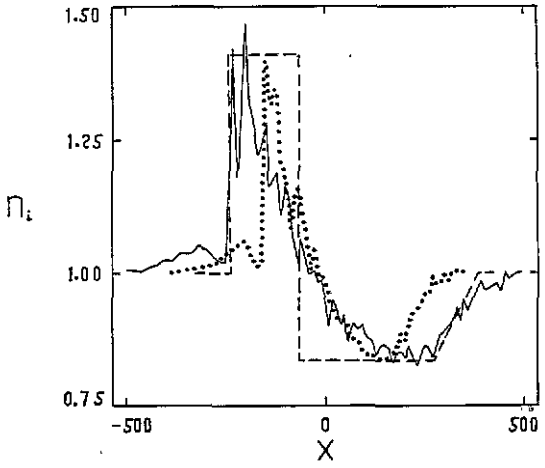

Figure 2. Ion density profiles from simulation with $T_{c0} = 0.001$, $T_{h0} = 1$ at $t = 128$ (dotted curve) and $t = 192$ (full curve). The broken line represents theoretical profile at $t = 192$.

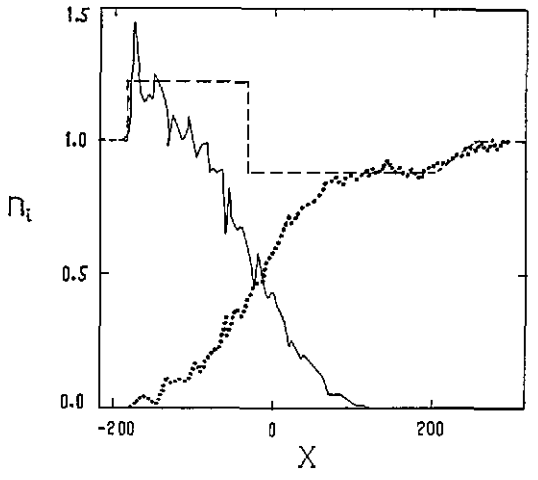

Figure 3. Cold ion density profile (full curve) and hot ion density profile (dotted curve) from simulation with $T_{c0} = 0.001$, $T_{h0} = 0.5$ at $t = 160$. The broken line represents the corresponding theoretical profile of the cold and hot ion density.

of ions reflected from the shock front (Moiseev and Sagdeev 1963), and presents a precursor of the following shock. The structure of the precursor has been well studied (Mason 1971, Gurevich *et al* 1989).

An example of the density profiles of both ion components is shown in combination with the corresponding theoretical profile in figure 3. The hot ions reach the shock and the cold ions penetrate to the plateau region. Again an acceptable correspondence between the simulation and theoretical profiles is exhibited outside the region in which the hot and cold ions are mixed together.

Potential profiles are similar to density profiles. This can be seen graphically in figure 4. A potential profile is so structured that the cold ions turn out to be accelerated toward the hot ions. Contrastingly, the hot ions come up against the

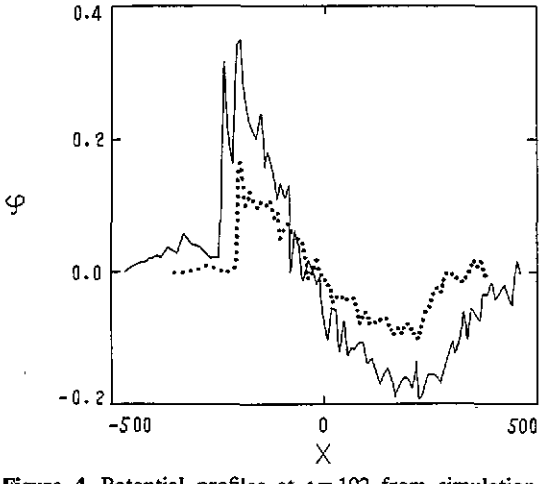

Figure 4. Potential profiles at $t = 192$ from simulation with $T_{c0} = 0.001$, $T_{h0} = 1$ (full curve) and $T_{c0} = 0.001$, $T_{h0} = 0.25$ (broken curve).

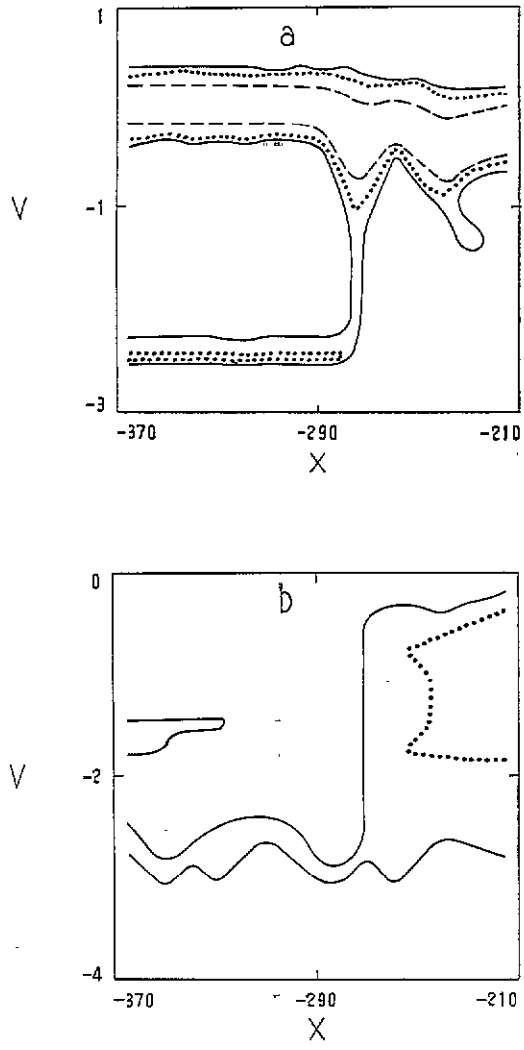

Figure 5. Contours of the constant numbers of simulation particles in the phase space at $t = 224$, $T_{c0} = 0.001$, $T_{h0} = 1$: (*a*) cold ions, (*b*) hot ions. Full, dotted and broken curves correspond to 1, 10 and 100 particles in a phase space cell, respectively.

potential barrier. Under these conditions the transition region between the shock and the plateau region can be considered as an expanding contact surface. In essence, two species of ions do not mix together outside this region. This is apparent from figures 3 and 5.

Figure 5 gives the phase spaces of the hot and cold ions. The shock front is located near the point $x \simeq -275$. Early in the development of the structure some of the hot ions traverse the potential barrier. In addition, the most energetic ions overcome the barrier. These two groups of the hot ions are seen in figure 5(*b*). For the most part, the hot ions lie behind the shock. There are cold ions reflected from the front of the shock. The velocity of reflected ions is about twice the shock velocity, as it should be. The reflected cold ions and the hot ions which are ahead of the shock front form the precursor observed in figures 2 and 4.

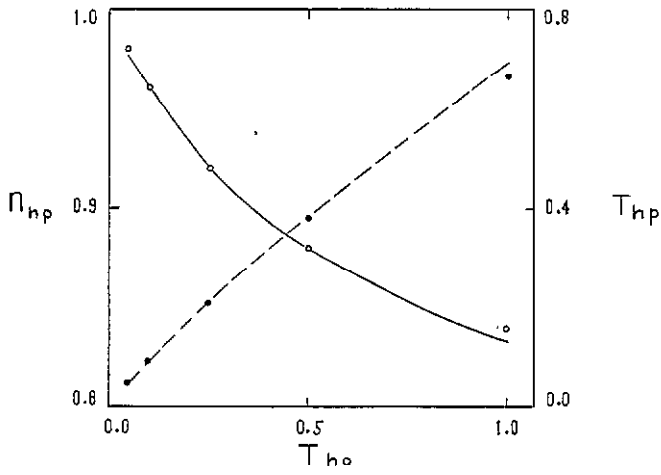

Figure 6. The hot ion density (full curve) and temperature (broken curve) at the plateau region as functions of T_{h0} derived from theory compared with the simulation data (open and full circles, respectively).

3.2. T_{h0} dependence

As stated above, the process is determined by the value of the initial hot ion temperature T_{h0}, if $T_{h0} \gg T_{c0}$. Let us consider the dependence of some quantities on T_{h0}.

In figure 6 are shown the hot ion density n_{hp} and temperature T_{hp} at the plateau region as functions of T_{h0}. Figure 7 gives the theoretical curves for n_{cp}, $V_p = V_{hp} = V_{cp}$ and w versus T_{h0} and the corresponding simulation data on V_{hp} and w. We see that the hot ion temperature and magnitude of velocity at the plateau region, the depth

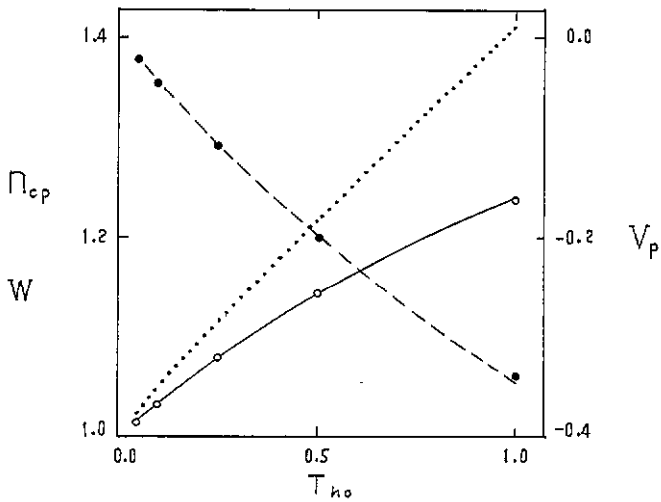

Figure 7. The shock speed (full curve) and ion velocity at the plateau region (broken curve) as functions of T_{h0} obtained from theory compared with the simulation data (open and full circles, respectively). The dotted curve represents the theoretical dependence of the cold ion density behind the shock on T_{h0}.

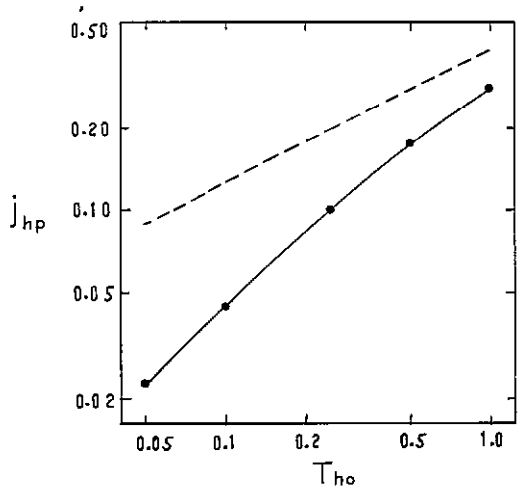

Figure 8. The hot ion current at the plateau region (full curve) as a function of T_{h0} obtained from theory compared with the simulation data (circles) and with the free-streaming flux (broken curve).

of density depression and the shock speed increase with a rise in the initial hot ion temperature T_{h0}. The figures show a good agreement between theory and simulation.

The theoretical analysis provides us with the values of V_{hp}, n_{hp} and T_{hp}. Given these quantities, we can estimate the values of ion current and kinetic energy flux at the plateau region. By assuming that the velocity distribution of the hot ions is Maxwellian with density n_{hp}, flow velocity V_{hp} and temperature T_{hp}, we obtain in terms of our normalized variables

$$j_{hp} = n_{hp} V_{hp} \qquad q_{hp} = n_{hp} V_{hp} (V_{hp}^2 + 3T_{hp}), \tag{39}$$

where j_{hp} and q_{hp} are the ion current and the kinetic energy flux at the plateau region, respectively.

Using theoretical dependence on T_{h0} of n_{hp}, V_{hp} and T_{hp}, we evaluate j_{hp} and q_{hp} as functions of T_{h0} from formulae (39). The absolute values of the quantities are presented in figures 8 and 9. These figures also demonstrate simulation data and free-streaming fluxes of particles j_0 and energy q_0 given by

$$j_0 \simeq 0.399 T_{h0}^{1/2} \qquad q_0 \simeq 0.798 T_{h0}^{3/2}.$$

Figure 8 shows a good fit of the theoretical curve to the values of current obtained by simulation. As for the energy flux, there is a minor difference between theory and simulation data. Note that we present averaged data and the spread of energy flux covers the theoretical curve.

4. Discussion

One of the most significant features of the decay of an ion temperature discontinuity is the fact that the compression wave arises from a compression of the cold ions rather than from a difference between the hot and cold ion fluxes crossing the contact surface. As discussed earlier, the last-mentioned difference is responsible for the formation of the density profile near the contact surface in a rarefied neutral gas.

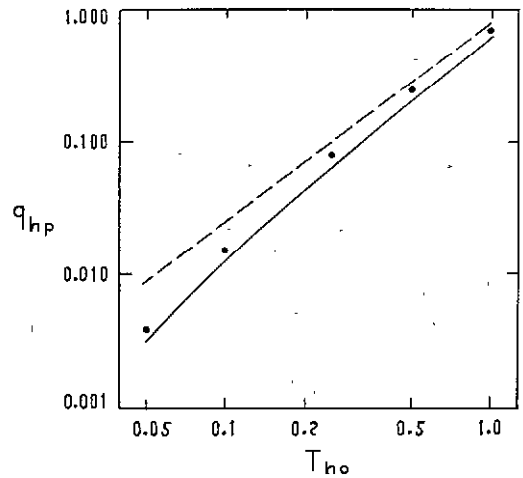

Figure 9. The hot ion energy flux at the plateau region (full curve) as a function of T_{h0} obtained from theory compared with the simulation data (circles) and with the free-streaming flux (broken curve).

In other words, the collisionless plasma behaves as a continuous medium rather than as a system of separate particles. This idea is also confirmed by the presence of typical hydrodynamic elements such as the plateau region and the rarefaction wave in the hot ion density profiles. Moreover, the numerical simulation supports the main results of the theory based on the continuous-medium approach.

The ion density in the wake of the shock falls substantially, and a plateau region occurs only for the hot ions. The density and potential profiles in the wake region are subjected to strong perturbations increasing with time (figures 2–4). The perturbations move at ion sound speed to the cold plasma side. Their growth is due to the interaction of the hot ion stream with ion sound waves in the non-isothermal plasma $T_{c0} \ll 1$. As is seen from figure 5, there is a two-stream velocity distribution behind the shock. The first stream is formed by the cold ions and the second one consists of the hot ions and has a wide spread of velocity. Some hot ions have velocities near the phase velocity of an ion sound wave and can transfer energy to the wave.

As already noted, the region behind the shock can be treated as an expanding contact surface. Since we consider neither hot nor cold plasma expansion, and because of this use the conditions at the contact surface whereby the density and current discontinuities must be formed, the theory cannot describe this region adequately. Even so, the theory and the simulation are in good agreement outside the expanding contact surface.

In a sense a similar case has already been considered in studies of the motion of a plasma with cold ions (Gurevich and Meshcherkin 1984). As we have mentioned in section 2, the concept of a self-similar expanding discontinuity together with relation (32) permits us to construct a full solution of the problem, if the structure of the discontinuity is of no interest. In our case the expanding contact surface plays the role of that discontinuity.

It is significant that we can eventually estimate some important quantities such as the shock speed and the ion current, energy flux, density and temperature of ions at the plateau region. Also we can describe the rarefaction wave.

5. Summary

In this paper we have considered the evolution of an initial ion temperature discontinuity in a collisionless plasma.

It has been found that a shock moves into the plasma with cold ions and a rarefaction wave does so into the plasma with hot ions, and the collisionless plasma behaves as a continuous medium rather than as a system of separate particles. The resulting potential dip slows down hot ions. The contact surface between the hot and cold ions expands. Ion sound waves are observed in the wake of the shock. The hot ion temperature and the magnitude of velocity at the plateau region, the depth of density depression and the shock speed, the ion current and the energy flux increase as the initial hot ion temperature increases. For all of the above values, good agreement exists between the particle simulation and the theoretical analysis.

Acknowledgment

The author would like to acknowledge Professor S I Anisimov for many fruitful discussions and for his cooperation in the early stage of the investigation.

References

Allen J E and Andrews J G 1970 *J. Plasma Phys.* **4** 187
Anisimov S I and Medvedev Yu V 1979 *Sov. Phys.–JETP* **49** 62
Baldwin D E and Logan B G 1979 *Phys. Rev. Lett.* **43** 1318
Braithwaite N St J, Montes A and Wickens L M 1981 *Plasma Phys.* **23** 713
Denavit J 1979 *Phys. Fluids* **22** 1384
—— 1981 *J. Comput. Phys.* **42** 337
Dimov G I, Zakaidakov V V and Kishinevsky M E 1976 *Sov. J. Plasma Phys.* **2** 326
Gitomer S J and Henderson D B 1979 *Phys. Fluids* **22** 364
Gurevich A V and Medvedev Yu V 1989 *Proc. XIX Int. Conf. on Phenomena in Ionized Gases* vol 1 (Belgrade) p 240
—— 1990 *Preprint* 26 (Moscow: FIAN)
—— 1992 *Preprint* 7-351 (Moscow: IVTAN)
Gurevich A V and Meshcherkin A P 1984 *Sov. Phys.–JETP* **60** 732
Gurevich A V, Pariiskaya L V and Pitaevskii L P 1966 *Sov. Phys.–JETP* **22** 449
Gurevich A V, Sagdeev R Z, Anisimov S I and Medvedev Yu V 1989 *Sov. Sci. Rev. A. Phys.* **13** (2) 1
Hatakeyama R, Suzuki Y and Sato N 1983 *Phys. Rev. Lett.* **50** 1203
Hockney R W and Eastwood J W 1981 *Computer Simulation Using Particles* (New York: McGraw-Hill)
Hultqvist B 1971 *Planet. Space Sci.* **19** 749
Ishiguro S 1987 *J. Phys. Soc. Japan* **56** 1354
Ishiguro S, Kamimura T and Sato T 1985 *Phys. Fluids* **28** 2100
Landau L D and Lifshits E M 1986 *Gidrodinamika* (Hydrodynamics) (Moscow: Nauka)
Liftshits E M and Pitaevskii L P 1979 *Fizicheskaya Kinetika* (Physical Kinetics) (Moscow: Nauka)
Malone R C, McCrory R L and Morse R L 1975 *Phys. Rev. Lett.* **34** 721
Mason R J 1970 *Phys. Fluids* **13** 1042
—— 1971 *Phys. Fluids* **14** 1943
Medvedev Yu V 1979a *Preprint* 3098 (Moscow: Kurchatov Institute for Atomic Energy)
—— 1979b *Pis'ma Zh. Tekh. Fiz.* **5** 200
Moiseev S S and Sagdeev R Z 1963 *J. Nucl. Energy* **C5** 43
Ohkawa T, Chu M S Hinton F L, Liu C S and Lee Y C 1983 *Phys. Rev. Lett.* **51** 2101
Sack Ch and Schamel H 1987 *Phys. Rep.* **156** 311
Sagdeev R Z 1966 *Reviews of Plasma Physics* vol 4 (New York: Consultants Bureau)
Temerin M, Cerny K, Lotko W and Mozer F S 1982 *Phys. Rev. Lett.* **48** 1175